HHS Public Access

Author manuscript

J Control Release. Author manuscript; available in PMC 2021 December 10.

Published in final edited form as:

J Control Release. 2020 December 10; 328: 696–709. doi:10.1016/j.jconrel.2020.09.050.

Incorporation of docosahexaenoic acid (DHA) enhances nanodelivery of antiretroviral across the blood-brain barrier for treatment of HIV reservoir in brain

Pengbo Guo[1], **Mengjie Si**[1], **Di Wu**[1], **Hui Yi Xue**[1], **Wenhui Hu**[2], **Ho Lun Wong**[3]

[1]School of Pharmacy, Temple University, 3307 North Broad Street, Philadelphia, PA USA 19140

[2]Lewis Katz School of Medicine, Temple University, Philadelphia, PA USA 19140

[3]School of Pharmacy, Temple University, 3307 North Broad Street, Philadelphia, PA 19140, USA.

Abstract

Although the newer antiretroviral (ARV) drugs are highly active against the human immunodeficiency virus (HIV) in the body compartment, they often fail to effectively tackle the HIV reservoir in the brain because of inefficient penetration to the blood-brain barrier (BBB). In this study, we investigated the potential benefits of incorporating docosahexaenoic acid (DHA), an omega-3 fatty acid essential for brain development, in lipid nanocarriers for facilitating the BBB passage of an ARV darunavir. The resulting nanocarriers (nanoARVs) containing 5–15% DHA were 90–140 nm in size, had high darunavir payload (~11–13% w/w), good stability and minimal cellular toxicity, and could be further decorated with transferrin (Tf) for Tf-receptor targeting. In BBB models of hCMEC/d3 cells, nanoARVs with higher DHA content achieved increased nanocarrier uptake and up to 8.99-fold higher darunavir permeation than free darunavir. In animals, nanoARVs were able to achieve 3.38–5.93-fold increase in brain darunavir level over free darunavir. Tf-conjugated nanoARVs also achieved significantly higher anti-HIV activity than free darunavir (viral titer 2 to 2.6-fold higher in latter group).Comparison of DHA incorporation and Tf-receptor targeting showed that while both strategies could enhance the cellular uptake and brain accumulation of the nanocarriers, DHA was more effective ($P<0.05$) for improving BBB permeation and brain accumulation of the darunavir payload. Substituting DHA with another oil noticeably reduced the cellular uptake of nanoARVs. Overall, this proof-of-concept study has supported the development of DHA-based nanoARVs as an effective, safe yet technically simple

corresponding author. Electronic address: ho-lun.wong@temple.edu.

CRediT author statement

Pengbo Guo: Methodology, Investigation, Formal analysis, Writing - Original Draft

Mengjie Si: Methodology, Investigation, Formal analysis, Writing - Original Draft

Di Wu: Methodology, Investigation

Hui Yi Xue: Methodology, Investigation, Writing, Supervision - Review & Editing

Wenhui Hu: Methodology, Resources, Supervision,

Ho Lun Wong: Conceptualization, Methodology, Formal analysis, Writing - Original Draft, supervision, project administration, funding acquisition

strategy to enhance brain delivery of darunavir and potentially other lipophilic ARVs for treatment of HIV reservoir.

Graphical Abstract

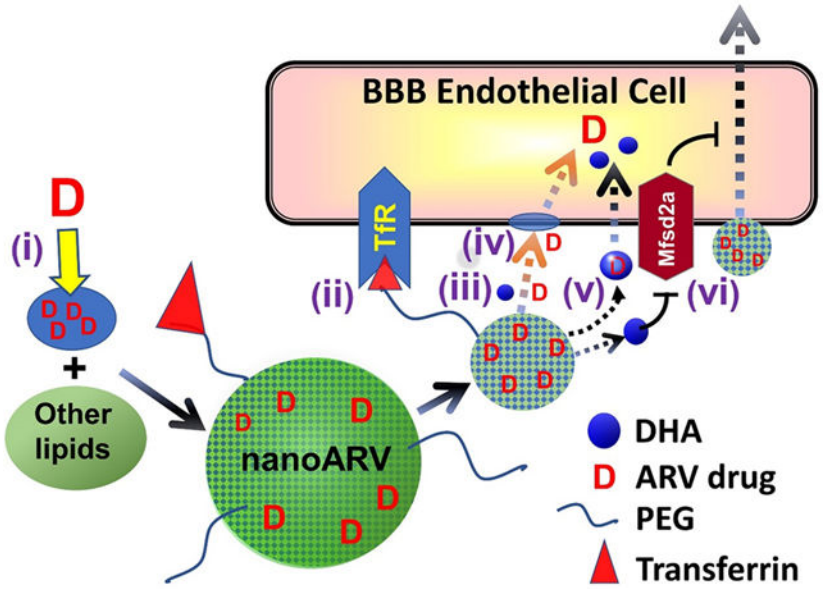

Keywords

Docosahexaenoic acid; nanocarriers; HIV; blood-brain barrier; antiretroviral; darunavir

1. Introduction

HIV tend to invade the blood-brain barrier (BBB) to form a major viral reservoir in the central nervous system (CNS) [1,2]. Not only this may lead to latent infections and antiretroviral (ARV) drug resistance [3–5], the HIV reservoir also persistently releases viral proteins to trigger a spectrum of debilitating and even deadly neurological complications known as HIV-associated neurocognitive disorders (HAND) [6]. In fact, HAND are reported as the most prevalent complication in HIV patients [7]. Almost as the sole treatment option for HAND, ARVs still often fail to eradicate the CNS HIV reservoir [5,8]. One key reason is that the BBB can limit the passage of many ARVs by its tight junctions and drug efflux transporters [9,10]. Hence, it is important to discover alternative strategies to enhance ARV delivery across the BBB.

Nanocarriers are known for their inherent abilities to enhance drug permeation across the BBB by promoting passive drug diffusion, endocytosis and transcytosis [9,11].Lipid-based nanocarriers are well-suited for ARV delivery because of their excellent biocompatibility and biodegradability [11,12]. Moreover, these nanocarriers can be conveniently surface-decorated with ligands, *e.g.* transferrin (Tf), to improve interactions with specific targets overexpressed at the BBB [13]. For instance, it was shown that solid lipid nanoparticles decorated with Tf demonstrated enhanced *in vivo* brain uptake. [14] In another study of

folate and lactoferrin modified liposomes carrying doxorubicin, researchers reported 2.69-fold higher brain uptake of doxorubicin than conventional liposomal doxorubicin. [15] Also considering that many ARVs are lipophilic molecules that can be efficiently entrapped in lipid-based nanocarriers [10,16], this class of nanocarriers are a reasonable choice to be used for brain delivery of ARVs.

Recently, it was found that brain nanodelivery can also be enhanced by incorporating certain brain nutrients [17,18]. Their low toxicity is especially appealing considering that nanotoxicity to the CNS can be a devastating issue [19,20]. The BBB also has intrinsic mechanisms to allow efficient passage of these nutrients. Docosahexaenoic acid (DHA) is an omega-3 fatty acid essential for proper brain development and functioning [21]. It is consumed as a dietary supplement on regular basis at large quantity and was shown to have neuroprotective functions [22,23]. This nutrient cannot be synthesized *de novo* in brain and must be imported from the systemic blood circulation, suggesting that it has at least one regular means to naturally cross the BBB. Recent studies revealed that DHA is actively imported into the CNS by a membrane transporter known as Mfsd2a that is exclusively expressed in the endothelium of the BBB microvessels [24]. Together, we see the strong potential of including DHA in nanocarriers to enhance the BBB permeation of lipophilic drugs such as ARVs with minimal risk of neurotoxicity.

In this proof-of-concept study, we developed DHA-based nanocarriers known as nanoARVs for delivering darunavir, a protease inhibitor shown to be highly effective for HIV treatment even when used as monotherapy [25]. Fig. 1 presents the design of Tf-nanoARV and summarizes the means potentially used by this nanocarrier to enhance BBB drug permeation (details in Discussion). Overall, this nanoformulation is designed to achieve the following: (i) Efficient solubilization and thus good loading of lipophilic ARVs like darunavir with the help of DHA. (ii) Enhanced drug transport across the BBB cell membrane as facilitated by DHA. (iii) Provide a robust platform to evaluate the feasibility of “dual-targeting” strategy by comparing the performance of no-Tf-nanoARV (nanoARV with DHA but without Tf conjugation) with Tf-nanoARV. Up to date, there have been only few reports on the conscious inclusion of DHA for brain nanodelivery, and this is the first report among them for enhanced ARV nanodelivery.

2. Materials and methods

2.1 Materials

The following materials were purchased from Avanti Polar Lipids (Alabaster, Alabama), including 1,2-distearoyl-sn-glycero-3-phosphocholine (DSPC), 1,2-distearoyl-sn-glycero-3-phosphoethanolamine-N-[methoxy(polyethylene glycol)-2000] (DSPE-PEG2000), 1,2-distearoyl-sn-glycero-3-phosphoethanolamine-N-[maleimide(polyethylene glycol)-2000] (ammonium salt) (DSPE-PEG(2000) Maleimide), cholesterol, 1,2-dioleoyl-sn-glycero-3-phosphoethanolamine-N-(lissamine rhodamine B sulfonyl) (DPPE-Rhod). Human holotransferrin (Tf), S-38 acetylthioglycolic acid N-hydroxysuccinimide ester (SATA). Hydroxylamine hydrochloride were purchased from Sigma-Aldrich.

2.2 Comparison of the performance of oils for darunavir solubilizaton

Various oils were mixed with excessive amount of darunavir powder and stirred overnight at room temperature. The mixtures were centrifuged to separate the oils saturated with the drug from any undissolved drug. The oils were diluted with ethanol or acetone and the darunavir concentrations were quantified using Spectramax M2 microplate reader at 266 nm. Oils without drugs served as baseline controls.

2.3 Preparation of transferrin conjugated DSPE-PEG2000-maleimide

Tf-conjugated phospholipid was prepared by coupling thiolated transferrin to DSPE-mPEG2000 maleimide phospholipid micelles. [26] The phospholipid micelles consisted of 1:4 molar ratio of DSPE-mPEG2000-maleimide and DSPE-mPEG2000 were prepared by thin-film hydration method. After drying with nitrogen, the phospholipid films were redissolved in 20 mM HEPES (35 mM NaCl, pH 7.3) at 65 °C. To prepare SATA-modified Tf, Tf and SATA at molar ratio of 1:8 were stirred for 45 min at room temperature in 20 mM HEPES buffer with 150 mM NaCl and 10 mM EDTA. Tf-SATA solution was mixed with 0.1 M hydroxylamine for 2 hr, and the mixture was passed through a PD-10 spin desalting column (pre-equilibrium with HEPES, NaCl pH 7.5, 0.1 mM EDTA) to remove the excessive SATA and hydroxylamine. Tf conjugation was then performed by stirring the mixture of SATA-modified Tf with DSPE micelle solution overnight at room temperature.

2.4 NanoARV preparation

All nanoARVs were prepared by solvent evaporation and emulsification technique using cholesterol, DSPC,DSPE-mPEG2000 at a molar ratio of 8:6:1 [27]. For Tf-nanoARV, some of the DSPE-mPEG2000 were substituted with Tf-DSPE-mPEG2000.To this mixture different quantities of DHA/drug were added to prepare a range of nanoARV formulations for subsequent studies. The final mixture dissolved in was blown dried with nitrogen, and the films formed were rehydrated with dichloromethane/biotech water mixture (1:10 by volume). The content was emulsified by vortexing for 30 seconds and sonicated for 5 minutes at room temperature. Nanoparticles were formed by evaporation of the volatile solvent at room temperature with constant stirring for 2 hr and then stored in vacuum overnight.

2.5 Evaluation of nanoARVs' size, morphology and DHA incorporation

Particle size and zeta potential values were measured by photon correlation spectroscopy (PCS) using Malvern Zetasizer NanoZS90 (Worcestershire, UK). All samples were diluted in deionized water and the measurements were conducted at 25 °C with refractive index set at 1.330 and medium viscosity at 0.89 mPa.s.

The morphology of nanoparticles was evaluated with cryogenic scanning electron microscopy (SEM) and transmission electron microscopy (TEM) using Apreo Scanning Electron Microscope (ThermoFisher Scientific, Waltham, MA) and JEOL F200 S/TEM (Peabody, MA), respectively. For SEM, nanoARV sample frozen in liquid nitrogen was transferred to the Quorum PP3010T cryogenic preparation chamber at a temperature of −140 °C, underwent sublimation at −90 °C, and sputtered with a thin layer of platinum prior to imaging at 2.00 kV. For TEM, a drop of nanoARV suspension (concentration: 0.5 mg/ml)

was placed on a 400-mesh copper grid (Ultra-thin carbon type A, Ted Pella Inc., Redding, CA). Samples were air-dried in the hood before examination at 120 kV.

To confirm the DHA added was well incorporated in nanoARVs, 4 hr and 48 hr after nanoparticle preparation, samples of nanoARVs were added to Vivaspin® 500 Centrifugal Concentrators (MWCO 100 kDa) and centrifugal filtration was performed for 30 min at 12,000 g. Any residual DHA not incorporated in nanoARVs was detected using Docosahexaenoic Acid ELISA Kit (MyBioSource, Inc. San Diego, CA).

2.6 Quantification of Tf conjugation efficiency, drug payload and drug encapsulation efficiency

To evaluate the conjugation efficiency of Tf on Tf-DSPE-mPEG2000, fluoresceinisothiocyanate (FITC)-labeled Tf was used as fluorescence marker. After conjugation reaction,the unconjugated Tf and free Tf-DSPE-mPEG2000 were separated from the phospholipidmicelles by centrifugal filtration at MWCO 100 kDa for 30 min at 12,000 g. Conjugation efficiency was calculated by measuring the fluorescence signal of FITC labeled Tf with Spectromax M2 microplate reader (Molecular Devices, Sunnyvale, CA).

The unencapsulated darunavir after preparation of nanoARV was removed by centrifugal filtration as described above. The entrapped drug in nanoARV was extracted with methanol. The extracted drug was quantified using Spectramax M2 microplate reader at 266 nm with blank nanoparticles served as the control. All measurements were performed in triplicate.

2.7 Analysis of nanoARV with differential scanning calorimetry (DSC)

DSC analysis of the nanoformulations was performed to evaluate the physical state of the nanocarrier and the encapsulated drug. Samples each containing 1–2 mg lyophilized Tf-nanoARV were weighed in aluminum pans, sealed, and equilibrated at 20 °C for 10 minutes. The analysis was performed using a DSC Q200 differential scanning calorimeter (TA Instruments, New Castle, DE) at a heating rate of 2 °C/min from 2 to 90 °C.

2.8 Studying drug and DHA release profiles

To study the darunavir release profiles, Tf-nanoARV or an equivalent amount of free darunavir was suspended in dialysis tubes (Tube-O-Dialyzer, Medi, MWCO 1kDa). Each sample assembly was placed in 25 ml of release medium (PBS at pH 7.2 with or without 1% w/v bovine serum albumin, BSA) at 37 °C under stirring. The volume of medium used has exceeded the manufacturer’s recommended standard for maintaining the sink conditions. At each selected time point, the release medium was sampled for LC-MS quantification (API4000 LC-MS/MS system, SCIEX, Framingham, MA) with equal amount of fresh medium replaced. Drug free medium and free darunavir served as negative and positive controls, respectively. The drug standard used for LC-MS was prepared using free darunavir dissolved in the release medium.

The release of DHA was studied using the above setting and conditions. DHA was quantified using Docosahexaenoic Acid ELISA Kit (MyBioSource, Inc. San Diego, CA) with free DHA dispersed in the release medium serving as the standard.

2.9 Dispersion stability and storage stability

To evaluate if the nanocarrier remained well-dispersed in serum-enriched environment, nanoARV samples were suspended in DMEM cell culture medium supplemented with 1% BSA at 37 °C. At each preselected time point, the size distribution of the nanocarrier samples was measured as previously described. For storage stability evaluation, Tf-nanoARV was stored in the glass vials filled with nitrogen and refrigerated for up to 30 days. At predetermined time points, samples were characterized for their size properties to monitor their stability.

2.10 Cell culture

Human cerebral microvascular endothelial (hCMEC/d3) cell line (purchased from Millipore sigma, Danvers, MA) was used as the model of human blood-brain barrier (BBB) function. This cell line is particularly suitable for this study due to its transferrin receptor expression [13]. The cells were plated out on cell culture dishes with a type I collagen coating and maintained in EndoGRO™-MV Complete Media supplemented with 1 ng/mL FGF-2 in a humidified incubator with 5% CO_2 at 37 °C. Cells were used after three passages of the primary culture until approximately 30 passages. Before using the hCMEC/d3 cells for the cellular uptake and drug permeation studies, Western Blot was performed and we confirmed the expression of transferrin receptor (*aka*. CD71) in the cells (see Supplemental Fig. 1) using metastatic prostate cancer cells as positive control (which demonstrated 10-fold expression *versus* normal cells [28]).

2.11 Evaluation of cellular toxicity of nanoARVs

MTT assays were performed to evaluate the nanoARV toxicity against hCMEC/d3 and 293T cell line (cell lines later used for anti-HIV activity assay). Subconfluent cells were seeded in 96-well microplates and grown for 24 hours. Suspension/solution of Tf-nanoARV, no-Tf-nanoARV or free darunavir containing 0 to 100 μM darunavir was added to the wells and incubated for another 24 hours at 37 °C. Drug-free nanocarriers and vehicle were used as negative controls, and 0.5% Triton-X 100 served as positive control. After 24 hr, 20 μl of 5 mg/mL MTT reagent was added to the wells and incubated for 2 hr. After the medium was removed, 150 μl of DMSO was added to each well. The absorbance of the colored dye produced was measured with Spectramax M2 microplate reader at 560 nm using 630 nm as reference.

2.12 Study cellular uptake of nanoARVs with fluorescence microscopy

Cellular uptake of nanoARVs was visualized with fluorescence microscopy. NanoARVs were prepared including fluorescent phospholipid 1,2-dioleoyl-sn-glycero-3-phosphoethanolamine-N-(lissamine rhodamine B sulfonyl). hCMEC/d3 cells were grown on poly-lysine treated coverslips in cell culture dish at standard cell culture conditions for two days. These cells were then treated with nanoformulations with different amounts of DHA

(5%, 15% w/w) and transferrin for 4 hours at 37°C. Free darunavir was used as control. Drug concentrations used in all groups were 1 mg/ml. At the end of treatment the nuclei of the cells were stained with DRAQ5 for 15 min. The treated and stained cells were washed with Dulbecco's phosphate-buffered saline (DPBS) 3 times and fixed with 4% formaldehyde for 15 min before getting examined with Axiostar Plus epifluorescence microscope (Carl Zeiss, Oberkochen, Germany). Images were captured with Insight camera model 8.0 and image analysis conducted using Spots Advanced imaging software (v.4.6, Diagnostic Instrument, Sterling Heights, MI).

2.13 Transepithelial transport of darunavir carried by nanoARVs

Transport of nanoARVs across the monolayer of hCMEC/d3 cells was evaluated using the transwell method. Collagen was used to pre-coat the cell culture inserts for at least 1 hr, followed by multiple washes using DPBS before seeding the hCMEC/d3 cells. The cells were incubated at 37 °C until confluent cell monolayer was formed. Lucifer yellow was added to monitor the integrity of the confluent cell monolayer. The drug as a nanoformulation or free drug was added to the apical side, and fresh medium was added to the basolateral side. After treatment for 1 or 6 hr, 150 μl sample was withdrawn from the basolateral side for drug quantification by LC-MS, and the same amount of fresh medium was added back to the well. The lucifer yellow was detected using Spectramax M2 microplate reader with excitation/emission wavelengths set at 428 nm/536 nm.

2.14 In vitro disease model and antiretroviral activity

Lentivirus and 293T cell line were engineered to constructing a recombinant retrovirus infected cell model [29]. Packaging vector, pCl-ECO plasmid, provided Gag-Pol polyprotein while the pCMV-VSV-G plasmid was used as envelope vector and GFP expression plasmid DNA used as a transfer vector. The mixture of these three plasmids was added to the target cells, and transfection was conducted using the calcium chloride transfection method. To study the antiretroviral activity of nanoARVs, free darunavir was used as a positive control while blank nanoARVs and vehicle were used as negative controls. After treatment, the supernatant was collected from each sample. The viral titer in the supernatants was measured using the Lenti-X p24 Rapid Titer Kit. Meanwhile, GFP expression associated with the expression of viral p24 protein can be visualized using fluorescence microscopy.

2.15 Evaluation of in vivo brain levels of darunavir and nanoARVs

All animal works were approved by Institutional Animal Care and Use Committee and animals were cared for in accordance with institutional guidelines. Mice (ICR, male and female equal ratio for brain drug level study, and male only for imaging) were purchased from Charles River Lab and housed in the Temple University Central Animal Facility for at least one week before any experiment. Mice were injected intravenously by tail-vein with 5 mg/kg (in terms of darunavir) of either Tf-nanoARV, no-Tf-nanoARV or free darunavir. Normal saline was used to adjust the tonicity and 1,1′-dioctadecyl-3,3,3′,3′-tetramethylindotricarbocyanine iodide was included in the nanoformulations as the fluorescence label. Mice were sacrificed after 24 hr of injection with the brains harvested for near infrared imaging. Odyssey® CLx Infrared Imaging System from LI-COR was used for near infrared (NIR) imaging. As quality control, prior to the above analysis the NIR signals

of the no-Tf and Tf-formulations at same concentrations were compared, no differences in their signal intensities were detected.

To compare the brain drug levels as delivered by different formulations, mice were randomized into several groups, and each was treated with either Tf-nanoARV, no-Tf-nanoARV or free darunavir at one dose per day for three consecutive days. At the end of each day selectedmice underwent perfusion as described by Lippi *et al* [30]. The heart was perfused with 0.9%saline and then 4% buffered paraformaldehyde (pH=7.4) once the blood ran clear. The fixedbrain tissues were harvested for LC-MS measurement of darunavir. For each gram of tissue, 2 mL of extracting solution (3:1 of PBS: acetonitrile by volume) was added for homogenization. The mixture was then ultracentrifuged under 150,000 g for 30 min. If the concentration of the supernatant was out of the linear range, the supernatant was either concentrated by vacuum centrifuge or diluted for LC-MS detection (API4000 LC-MS/MS system, SCIEX, Framingham, MA). The data of vehicle-treated animal brains served as the baseline control.

2.16 Statistical analysis

Unless otherwise specified, for multiple group studies, data analysis used one-way ANOVAs with post-hoc Tukey's test for selected group comparison. For two-group comparison, Student's t-tests (larger samples) or Mann-Whitney U-test (smaller samples) were performed. $P<0.05$ was considered significant.

3 Results

3.1 Drug solubilization and physicochemical characterization of nanoARVs

Table 1 shows the solubilities of darunavir in a number of oils commonly used in pharmaceuticals. Among them Capmul MCM C8 demonstrated the highest solubility of darunavir, followed by DHA. The drug solubilities in the remaining oils were only a fraction of Capmul and DHA. We thus studied nanocarrier formulations using these two oils and two other solid lipids (cholesterol and tripalmitin). In comparison, the two prepared with Capmul appeared smaller but had noticeably higher polydispersity index (PDI) indicating broader size distribution. The PDI values of both DHA-based nanocarriers were significantly lower ($P<0.05$). Capmul was thus only used for comparison instead of serving as the primary option for nanoARV preparation.

The impact of two key parameters, DHA content and amount of darunavir (*i.e.* drug loading), on the average size and PDI of the resulting nanoARVs was shown in Figs. 2A (left and right panel, respectively). Overall, the size of nanoARV (before Tf conjugation) was in the range of 90–140 nm and was positively with the DHA content and darunavir loading ($P<0.05$). In terms of PDI, narrow size distribution (<0.2) were obtained when the DHA content was at 15% w/w.We therefore considered 15% DHA, 15% intended payload (marked as X in the figures) desirable and this was used as the primary composition in the subsequent experiments. The DHA content also appeared to enhance darunavir encapsulation (Fig. 2B). The drug encapsulation efficiency was improved from 28.2% when there was no DHA to 55.4% at 5% DHA content, to 72.5% at 20% DHA. To learn if DHA

was also well entrapped in nanoARVs, Fig. 2C presents the unentrapped DHA after preparation and storage.1 hr and 48 hr after preparation, 0.11% and 0.14% (by weight of nanoparticles, same below) were detected in nanoARV loading 5% DHA, and 0.25% and 0.22% detected in nanoARVs with 15% DHA, respectively. In other words, nearly all of the DHA added in the preparation was efficiently incorporated as a part of the resulting nanoARVs, and there was no sign of significant leak of DHA from the nanocarrier after 48 hr of storage.

Fig. 2D present the SEM and TEM images (left and right panel, respectively). The nanoparticles were spherically shaped and the size around 100 nm, which was generally consistent with the PCS measurements. The TEM image revealed compact structure that resembled nanosphere instead of liposomes or vesicles.

Fig. 2E presents the DSC thermograms of nanoARV, physical mixture of phospholipid/lipid ingredients/darunavir powder, and darunavir powder only. Both nanoARV and the lipids/drug mixture did not show the darunavir peak, indicating that the drug was in solubilized or amorphous state likely due to the solubilizing effect of DHA. Comparison of nanoARV to lipids/drug mixture shows that the former required much less energy for phase transition. This suggests that the crystallinity of the solid lipid ingredients in nanoARV was also reduced after nanocarrier formation.

3.2 Transferrin conjugation

The various effects of Tf conjugation on the resulting Tf-nanoARVs are presented in Figs. 3A–D. Fig. 3A shows that the efficiency of Tf conjugation remained consistently about 90% regardless of the Tf to lipid ratio tested. Tf conjugation also did not significantly affect the size of the resulting nanoARVs. The size of all Tf-nanoARVs fell within 80–120 nm range with no significant differences among them (Fig. 3B). The levels of darunavir payload remained high and were not affected by Tf conjugation (Fig. 3D); the darunavir payloads of Tf-nanoARVs with different Tf ratios were within the range of 11–13% w/w. The PDI value (indicating the size distribution) was the only parameter that was noticeably affected (Fig. 3C). It was lowest (~0.2) when the lipid to Tf ratio was 12:1. However, the effect was not statistically significant ($P>0.05$).

3.3 Studies of drug encapsulation and drug/DHA release

Figs. 4A–E present the various release profiles. Figs. 4A–D show the impact of various formulation factors on the darunavir release from nanoARVs. Higher DHA content was shown to increase the total amount of drug release after a few days (Fig. 4A), but the initial release in the first few hours (Fig. 4B) was noticeably higher with lower DHA content, suggesting that the entrapped DHA may facilitate darunavir release but also help to avoid reduce the burst release effect. Fig. 4C presents the drug release from Tf-nanoARVs and no-Tf-nanoARV in release buffer with or without bovine serum (1 %w/v BSA). Both formulations showed similarly controlled drug release behaviors and were able to release >80% of their darunavir payloads (no statistical difference). The impact of Tf conjugation and the presence of serum was minimal.

The extent of PEGylation also affected the darunavir release behaviors. We typically used 6.7 % PEG-lipids by weight of nanoARV, but Fig. 4D shows that a higher level of PEGylation could further slowed down the drug release. By increasing the PEG level to 15%, the initial drug release could be decreased to about 20% in 4 hours and about 40% in 24 hours.

The DHA content in nanoARVs was also released (please note that this is at 37 °C in release buffer, in Fig. 2C nanoARVs were stored in stock at 4 °C), but considerably slower than darunavir. After 5 days only 27.6% of the DHA in nanoARVs was released.

3.4 Stability and cellular toxicity evaluation

We first evaluated the dispersion stability of Tf-nanoARV in an environment simulating physiological conditions (buffer supplemented with 1% BSA at 37 °C). The particle size and PDI both increased and the zeta potential reduced during the 5-day study (Figs. 5A), but the increases were moderate. The average size increased from about 95 nm to 110 nm, and PDI value increased from about 0.22 to 0.33. The size and zeta potential stability of the Tf-nanoARV stock suspension was also monitored at 4 °C (Fig. 5B). Only marginal changes were observed. Overall, nanoARVs remained well dispersed without substantial aggregation in protein-rich medium or when stored in refrigerator.

Then we evaluated if nanoARV caused undesirable toxicity to the target cells. Fig. 5C shows that no significant loss in the viability in both BBB endothelial cells hCMEC/d3 (left) and 293T (right) cells with both Tf-nanoARV and no-Tf-nanoARV at most of the nanoARV concentrations. The toxicity to hCMEC/d3 cells was minimal up to 50 μM drug level, and significant ($P<0.05$) but only modest reduction in cell viability at 100 μM when compared to vehicle-treated cells. For information, IC50 of duranavir: 1.0–8.5 nM [31]. The nanoARV formulation can thus be considered non-cytotoxic when used within or even modestly higher than the therapeutic concentration range.

3.5 Cellular uptake of nanoARVs and drug permeation across hCMEC/d3 cell model

Figs. 6A–C present the fluorescence images showing the uptake and distribution of various nanoARVs (in red) in hCMEC/d3 cells (nuclei in green). The impact of two parameters was evaluated: the DHA level and Tf level in nanoARVs. The two panels (Figs. 6A–B) refer to the images of nanoARVs incorporating 5% DHA and 15% DHA, respectively, and in each panel four different Tf levels (0, 1:40, 1:20, 1:10 in terms of Tf to lipid ratio w/w) were studied. In general, the BBB endothelial cells took up all four 15% DHA nanoARV formulations more efficiently than their 5% counterparts (note the red fluorescence). We also tested similar nanoparticles by substituting DHA with other oils, *e.g.* Capmul MCM, but no noticeable intracellular fluorescence was detected at both 5% and 15% level (Fig. 6C). This confirmed the significance of DHA for enhancing cellular uptake. In Figs. 6A and B, it was also shown that the cellular nanoARV uptake tended to increase with higher Tf ratio and this effect was particularly evident in the 5% DHA group. Overall, both DHA and Tf levels contributed to cellular nanoARV uptake at *in vitro* level.

Transwell assay was performed to measure permeation of darunavir across the BBB model. The barrier integrity has been confirmed using Lucifer yellow. Fig. 6D shows that all four

nanoARV formulations (no-Tf-nanoARV or Tf-nanoARV, each containing 5% or 15% DHA) led to significantly ($P<0.05$ to $P<0.01$) enhanced darunavir permeation across the cell barrier relative to the free drug. After 1 hr, the amounts of permeated drug for no-Tf-nanoARV (5% DHA), Tf-nanoARV (5% DHA), no-Tf-nanoARV (15% DHA) and Tf-nanoARV (15% DHA) were 2.15-, 2.16-, 3.95- and 5.92-fold of the free darunavir group, respectively. After 6 hr, the amounts of permeated drug recovered in the same order were 3.16-, 3.21-, 7.67- and 8.99-fold of the free darunavir group, respectively. In terms of absolute value, the highest amount of darunavir recovered in the recipient chamber was 47.3% of the dose added to the donor chamber in Tf-nanoARV (15% DHA) group.

It should be noted that the drug permeation enhancement appeared to be contributed mostly by DHA (comparing 5% DHA to 15% DHA: $P<0.05$ at 1 hr; $P<0.01$ at 6 hr), and the effect achieved by Tf conjugation was modest and not significant ($P>0.05$). When the DHA level in nanoARVs was 15%, over 40% of the loaded darunavir could cross the cellular barrier after 6 hr in the presence of Tf decoration or not.

3.6 Improving anti-HIV activities with nanoARVs

We evaluated the anti-HIV activities using stably transfected 293T cells expressing p24 HIV capsid protein. In these cells, GFP served as the reporter gene product which indicated p24 expression. The images (Fig. 7A) showed that both Tf-nanoARV and free darunavir achieved strong suppression of the capsid protein expression. Drug-free Tf-nanoARV apparently did not demonstrate anti-HIV activities. The cells treated with the blank nanocarrier control remained highly active in expressing the HIV protein like the vehicle control.

The quantitative result of viral protein titer assay was presented in Fig. 6B. Tf-nanoARV demonstrated higher activity ($P<0.05$) over free darunavir in all concentrations tested. At all three drug levels (50, 100 and 200 nM), the viral protein titers produced after free darunavir treatment were 2 to 2.6-fold higher than the Tf-nanoARV group at the corresponding darunavir levels. We also performed the assay using drug-free Tf-nanoARVs, several order higher viral titers were observed with no significant difference compared with the vehicle control. The result showed that at same drug concentration, Tf-nanoARV achieved superior anti-HIV activity than the free drug, and this activity was mainly derived from the drug loaded in the nanoformulation, not from the lipid nanocarrier itself.

3.7 nanoARVs achieved enhanced in vivo nanocarrier and darunavir accumulation in brain

The *in vivo* darunavir concentration in brain was monitored for three consecutive days and the data shown in Fig. 8A. Both nanoARV formulations (Tf- or no-Tf) led to significantly higher brain darunavir levels than the free drug group in all three days. The improvements of brain darunavir level over the free drug were 5.93-, 3.96-, 3.38-fold using Tf-nanoARV and 4.65-, 3.97-, 4.41-fold using no-Tf-nanoARV on day 1, 2 and 3, respectively.

The nanocarrier distribution in brain was evaluated using near infrared (NIR) fluorescence imaging. Fig. 8B presents the images of the brains treated with no-Tf-nanoARVs or Tf-nanoARVs labeled with an NIR dye. The intrinsic NIR fluorescence of the tissue was shown

in red and the fluorescence of nanoARVs in green. The overlay (left, brain + nanoARVs) and green only (middle, nanoARVs only) images are presented. The images showed that both nanoARV formulations noticeably accumulated in the animal brains. After subtraction of the background green signal of the control, analysis of the green color intensity using ImageJ software showed that the relative intensity per pixel of no-Tf-nanoARV group *versus* Tf-nanoARV group was 1.0±0.33 to 1.41±0.51 (right, Fig. 8B). Tf-nanoARV was moderately but significantly better accumulated in the brain than no-Tf-nanoARV ($P<0.05$).

In all of the animals tested, none of the them manifested any gross signs of acute toxicity and distress such as significant weight loss (>10%), physical inactivity and fur roughing.

4. Discussion

Efficient and safe delivery of drug across the BBB is critical for drug therapy of HAND which requires sufficiently high ARV levels in the CNS compartment for eradication of the latent and sometimes drug-resistant HIV strains [32, 33]. DHA as an essential brain nutrient is an appealing choice to prepare safe, efficient lipid-based nanocarriers for this purpose. This study focuses on exploring the impact of DHA incorporation on nanodelivery of ARV across the BBB. Overall, our results indicate that this approach provides benefits in several aspects.

The first benefit is solubilization of darunavir (Table 1). With the drug in solubilized state, it was expected to get better dispersed in the nanocarriers and thus more efficiently entrapped. This is supported by the data in Fig. 2B, which show nearly 2-fold improvement in darunavir encapsulation when the DHA content was increased from 0 to 15%. There was a concern that this may unfavorably increase the nanocarrier size, but our data (Fig. 2A) showed that at 15% DHA, nanoARVs remained reasonably small (around 110 nm) with narrow distribution (PDI around 0.2), which is in the size range of clinically used nanoformulations such as Abraxane (130 nm) and Doxil (85 nm) [34].

The TEM image of nanoARVs (Fig. 2D) revealed compact appearance with 15% DHA loaded, while the DSC thermogram indicated that the drug and lipid content in nanoARVs was not in crystalline state (Fig. 2E). Both suggested that the oil and drug were finely ore even molecularly dispersed in the lipid core without forming micro-compartments or aggregates there. The nanoARV's structure thus resembles nanostructured lipid carriers (NLC) in which the dispersed oil molecules introduce amorphosity to the solid lipids and the entrapped drug [12,35]. But unlike the prototypical NLC which include more hydrophobic solid lipids or waxes, often exceed 200 nm and are ideal for topical application [36,37], the high phospholipid content in nanoARVs ensures easy emulsification into finer particles and good stability in serum-rich environment and during storage (Fig. 5). NanoARV can therefore be considered a modified, stable version of NLC suitable for systemic use.

After showing that DHA can improve drug solubilization, modify nanoparticle structure and increase drug encapsulation, we focused on learning the role of the entrapped DHA in modifying the drug release and BBB permeation behaviors. Consistent with the general characteristics of NLC, the high amorphosity of nanoARVs caused by DHA likely have

reduced the poorly controlled surface deposition of darunavir and hence the initial burst release (note: compare 0% DHA *vs* 15% DHA profiles in Fig. 4B) so less drug will be lost to the circulation before the nanoARVs reach the brain target. In addition, higher DHA content also led to more complete drug release (at 120 hr, 88.4% *vs* 55.7% cumulative release comparing 15% DHA *vs* 0% DHA, Fig. 4A), the drug release process was evidently facilitated by the increasing DHA level.

Regarding BBB drug permeation, we separated this into two stages: drug uptake into the BBB endothelial cells and leaving their basolateral side to complete the BBB passage [38]. By comparing the images between the 5% DHA-nanoARV with 15% DHA-nanoARV at the corresponding Tf ratio (Figs. 6A and B), it is evident that higher DHA level could enhance both cell surface accumulation and cellular internalization of nanoARVs. This effect was most obvious in the absence of Tf (No Tf, compare the red panels in Figs. 6A and B), 5% DHA-nanoARVs were barely detectable while 15% DHA-nanoARV distributed extensively on the surface of all cells and in some cells' cytoplasm. This benefit of DHA was verified by comparing with nanoARVs made of other oils (*e.g.* Capmul MCM), which achieve very low intracellular fluorescence at both oil levels (5% and 15%, Fig. 6C). This was not a misleading result caused by staining of dead cells as shown by the low cytotoxicity data (Figs. 5C and D), a finding not surprising considering the regular role of DHA being a cytoprotective nutrient [37].

Fig. 6D showed significant permeation enhancing effects using both no-Tf-nanoARV and Tf-nanoARV with 15% DHA. Both formulations achieved passage of over 40% of darunavir across the cell barrier after 6 hr, equivalent to 7.67- and 8.99-fold of the free darunavir group, respectively. Although the 5% DHA-nanoARVs also improved darunavir permeation (2.15- and 2.16-fold over free darunavir using no-Tf-nanoARV and Tf-nano-ARV, respectively), their enhancements were significantly ($P<0.05$) lower than the 15%-DHA counterparts. In comparison, the enhancements brought by Tf-conjugation were modest and not significant ($P>0.05$).In short, the data indicated that while both DHA and Tf-receptor targeting improved cellular uptake of nanocarriers, DHA played a more crucial role than Tfin facilitating darunavir permeation across the BBB model.

After showing that nanoARVs enhanced or at least preserved the anti-HIV activities of darunavir *in vitro* (Fig. 7A and B, 2–2.6 fold reduction in viral protein levels *vs* free drug, $P<0.05$), we proceeded to *in vivo* evaluation. Fig. 8A showed 3.38- to 5.93-fold increase in darunavir concentration in nanoARV treated animal brains *versus* the corresponding free drug groups. This benefit was consistent from 1 day to 3 days of treatment. Similar to the drug permeation assay data, Tf conjugation did not lead to higher drug accumulation in the brain. Interestingly, the result about the nanoARV levels in brain (Fig. 8B) showed results that have apparently contradicted to the brain drug level data. While no-Tf-nanoARV and Tf-nanoARV both distributed extensively in the brains, the latter formulation was better accumulated.

If we consider the *in vitro* and *in vivo* results together, the trend shown in the *in vivo* drug data apparently resembles that of the *in vitro* drug permeation, whereas the trends about the *in vivo* nanocarrier brain levels and *in vitro* cellular nanoARV uptake are similar. It is thus

possible that DHA in nanoARVs enhanced both uptake into the endothelial cells and permeation of the darunavir payload across the barrier, while Tf-receptor targeting mainly facilitated the first step.

Considering the promising effects of DHA for enhancing brain drug nanodelivery, it is surprising that so far few researchers have intentionally exploited this benefit. There were indeed reports of DHA-incorporated delivery platforms. For instance, Guerzoni *et al* developed a dual-drug carrier delivering DHA/curcumin combination [23] and showed that it promoted the neuronal survival and repair processes. Mulik *et al* studied low-density lipoprotein nanoparticles reconstituted with DHA and demonstrated neuroprotective effects in mice brains [39]. Loughrill *et al* also developed microencapsulated formulations of DHA and showed improved DHA uptake [40]. However, in these studies DHA was included mainly for its neuroprotective or nutritional role and not for brain nanodelivery. In Mulik *et al*'s study they did demonstrate increased local accumulation of DHA in brain, but they had applied focused ultrasound which is a well-established physical method to transiently permeabilize the BBB [39], so it is difficult to confirm if DHA was responsible for the enhanced brain delivery in this study.

One exception was the development of DHA-functionalized block co-polymer micelles by Shao *et al* [41]. It was reported that DHA functionalization significantly improved the delivery of itraconazole, an antifungal that poorly penetrates the CNS. In this study, they suggested increased cell surface binding of DHA to glucose transporter-1 (GLUT-1) as the cause of enhanced cellular uptake of the micelles. Unlike this micellar system in which the DHA molecules were directly immobilized to the micellar surface by conjugation, in nanoARVs the DHA content was in free form, so it is unclear if the two DHA-incorporated carriers shared the same BBB-targeting mechanism.

Overall, the mechanism for the observed enhanced nanodelivery caused by DHA-based nanoARVs is likely complex and deserves a specialized study that is beyond the scope of this report. However, the present data still allow us to develop some hypotheses as summarized in the scheme in Fig. 1. We have already discussed good drug encapsulation, feasibility to work together with another active targeting mechanism (*e.g.* Tf-receptor) and improved drug release performance. As DHA was shown to get released (Fig. 4E), this released DHA may also have played a supportive role. It should be noted that about 3 times of the encapsulated darunavir *versus* DHA got released (Fig 4A *vs* 4E), so the majority of the released drug molecules were not in form of “drug in DHA nanodroplets” as initially expected. However, as a polyunsaturated oil, Any released DHA can still serve as an enhancer of the fluidity and flexibility of cell membrane lipid bilayers to facilitate drug passage [42]. This function of DHA has been demonstrated in topical applications [43]. Besides, DHA has long been recognized for their inhibitory effect on P-glycoprotein (P-gp) in cancer, *e.g.* reversing paclitaxel resistance by inhibiting P-gp in ovarian cancer cells [44]. Recent studies showed that the P-gp in BBB endothelial cells can also be inhibited by DHA [45]. This may also contribute to the enhanced darunavir permeation as darunavir is also a P-gp substrate [46]. This issue deserves more investigation in future.

It is also possible that DHA may modulate other BBB transport mechanisms. Besides binding to the aforementioned target GLUT-1, Mfsd2a is another potential target that DHA may exploit [47]. As some DHA was also released from nanoARVs, a portion of the released darunavir may associate with the DHA and be transported by these active pathways. Besides the DHA transport function, Mfsd2a also has innate suppressive effects on BBB transcytosis [48]. There is possibility that a high local level of DHA may have served as an inhibitor to block this function, essentially de-inhibits the transcytosis at the BBB. However, it should be noted that Mfsd2a was shown to mediate the transcytosis suppression by flipping DHA molecules to the membrane bilayer to disrupt caveolae formation [49], so clearly more in depth mechanistic studies are needed to delineate the exact nature of DHA-Mfsd2a interactions in this process.

Finally, our early data of biodistribution analysis are shown in Supplemental data (Fig. S2). They showed higher levels of darunavir in liver and spleen when delivered using nanoARVs *versus* free drug. Meanwhile, in the new data the brain drug levels achieved by nanoARVs remained several fold higher than the free drug group. This finding has confirmed the benefit of nanoARVs in terms of brain delivery, while suggesting that there is room for more optimization of the nanoformulation especially in the area of further reducing the reticuloendothelial clearance, thus strengthening this effective, safe and yet technically simple DHA-based approach to overcome the BBB.

5. Conclusion

Strategies to achieve efficient drug permeation across the BBB at minimal risk of neurotoxicity have been much pursued in the field of nanodelivery. This is a particular concern for treatment of HAND which requires sufficient antiviral drug level in the CNS compartment to tackle the HIV reservoir there. In this study, we investigated the potential benefits of incorporating DHA, an essential brain nutrient with neuroprotective properties, in lipid-based nanocarriers for facilitating the BBB passage of an ARV darunavir. Our results showed that nanoformulations of darunavir, known as nanoARVs, with higher DHA content achieved substantially higher uptake by the BBB endothelial cells as well as animal brains. This translated well into multi-fold enhancement in the permeation of darunavir across the BBB model and brain drug accumulation *in vivo*. In comparison, Tf-receptor targeting as a more established brain targeting strategy was also shown effective in facilitating cellular uptake and brain distribution of the nanocarriers, but could only lead to modest improvement in carrying their darunavir payload across the BBB. As expected, no toxicity was observed in the cell models and animals treated with the DHA-based nanoformulations. Overall, our findings in this proof-of-concept validate the benefits of incorporating DHA in nanocarriers as an effective, simple and likely safe strategy to enhance brain delivery of darunavir and potentially other lipophilic compounds.

Supplementary Material

Refer to Web version on PubMed Central for supplementary material.

ACKNOWLEDGEMENT

The study was supported by National Institute of Health/ National Institute of Neurological Disorders and Stroke R03 grant (R03NS112078).

ABBREVIATIONS

ARV	antiretroviral
BBB	blood brain barrier
CNS	central nervous system
DHA	docosahexaenoic acid
DSC	differential scanning calorimetry
DSPC	1,2-distearoyl-sn-glycero-3-phosphocholine
DSPE-mPEG2000	1,2-Distearoyl-*sn*-glycero-3-phosphoethanolamine-N-[methoxy(polyethylene glycol)-2000]
FITC	fluorescein isothiocyanate
HAND HIV	associated neurocognitive disorders
HIV	human immunodeficiency virus
HPLC	high performance liquid chromatography
MTT	(3-(4, 5 dimethylthiazolyl-2)-2, 5-diphenyltetrazolium bromide)
NIR	near infrared
NLC	nanostructured lipid carrier
PDI	polydispersity index
SATA	S-38 acetylthioglycolic acid N-hydroxysuccinimide ester
SEM	scanning electron microscope
TEM	transmission electron microscope
Tf	transferrin

REFERENCES

[1]. Wallet C, De Rovere M, Van Assche J, Daouad F, De Wit S, Gautier V, Mallon PWG, Marcello A, Van Lint C, Rohr O, Schwartz C, Microglial Cells: The Main HIV-1 Reservoir in the Brain, Front Cell Infect Microbiol. 9 (2019) 362. [PubMed: 31709195]

[2]. Li GH, Henderson L, Nath A, Astrocytes as an HIV reservoir: Mechanism of HIV Infection, Curr HIV Res. 14 (2016) 373–381. [PubMed: 27719663]

[3]. Fischer-Smith T, Croul S, Sverstiuk AE, Capini C, L'Heureux D, Régulier EG, Richardson MW, Amini S, Morgello S, Khalili K, Rappaport J, CNS invasion by CD14+/CD16+ peripheral blood-derived monocytes in HIV dementia: perivascular accumulation and reservoir of HIV infection, J Neurovirol. 7 (2001) 528–541. [PubMed: 11704885]

[4]. Mikhailova A, Valle-Casuso JC, Sáez-Cirión A, Cellular Determinants of HIV Persistence on Antiretroviral Therapy, Adv Exp Med Biol. 1075 (2018) 213–239. [PubMed: 30030795]

[5]. Clutter DS, Jordan MR, Bertagnolio S, Shafer RW, HIV-1 drug resistance and resistance testing, Infect Genet Evol. 46 (2016) 292–307. [PubMed: 27587334]

[6]. Ferrell D, Giunta B, The impact of HIV-1 on neurogenesis: implications for HAND, Cell Mol Life Sci. 71 (2014) 4387–4392. [PubMed: 25134912]

[7]. Eggers C, Arendt G, Hahn K, Husstedt IW, Maschke M, Neuen-Jacob E, Obermann M, Rosenkranz T, Schielke E, Straube E, German Association of Neuro-AIDS und Neuro-Infectiology (DGNANI), HIV-1-associated neurocognitive disorder: epidemiology, pathogenesis, diagnosis, and treatment, J Neurol. 264 (2017) 1715–1727. [PubMed: 28567537]

[8]. Sung JM, Margolis DM, HIV Persistence on Antiretroviral Therapy and Barriers to a Cure, Adv Exp Med Biol. 1075 (2018) 165–185. [PubMed: 30030793]

[9]. Wong HL, Wu XY, Bendayan R, Nanotechnological advances for the delivery of CNS therapeutics, Adv Drug Deliv Rev. 64 (2012) 686–700. [PubMed: 22100125]

[10]. Wong HL, Chattopadhyay N, Wu XY, Bendayan R, Nanotechnology applications for improved delivery of antiretroviral drugs to the brain, Adv Drug Deliv Rev. 62 (2010) 503–517. [PubMed: 19914319]

[11]. Tsou YH, Zhang XQ, Zhu H, Syed S, Xu X, Drug Delivery to the Brain across the Blood-Brain Barrier Using Nanomaterials, Small. 13 (2017) 43.

[12]. Garg B, Beg S, Kumar R, Katare OP, Singh B, Nanostructured lipidic carriers of lopinavir for effective management of HIV-associated neurocognitive disorder, J Drug Deliv Sci Tech. 53 (2019) 53:101220.

[13]. Johnsen KB, Burkhart A, Thomsen LB, Andresen TL, Moos T, Targeting the transferrin receptor for brain drug delivery, Prog Neurobiol. 181 (2019) 10166.

[14]. Gupta Y, Jain A, Jain SK, Transferrin-conjugated solid lipid nanoparticles for enhanced delivery of quinine dihydrochloride to the brain, J Pharm Pharmacol. 59 (2007) 935–940. [PubMed: 17637187]

[15]. Vyas TK, Shahiwala A, Amiji MM, Improved oral bioavailability and brain transport of Saquinavir upon administration in novel nanoemulsion formulations, Int J Pharm. 347 (2008) 93–101. [PubMed: 17651927]

[16]. Chattopadhyay N, Zastre J, Wong HL, Wu XY, Bendayan R, Solid lipid nanoparticles enhance the delivery of the HIV protease inhibitor, Atazanavir, By a human brain endothelial cell line, Pharmaceutical Research. 25 (2008) 2262–2271. [PubMed: 18516666]

[17]. Sánchez-Navarro M, Giralt E, Teixidó M, Blood-brain barrier peptide shuttles, Curr Opin Chem Biol. 38 (2017) 134–140. [PubMed: 28558293]

[18]. Jafari B, Pourseif MM, Barar J, Rafi MA, Omidi Y, Peptide-mediated drug delivery across the blood-brain barrier for targeting brain tumors, Expert Opin Drug Deliv. 16 (2019) 583–605. [PubMed: 31107110]

[19]. Viswanath B, Kim S, Influence of nanotoxicity on human health and environment: The alternative strategies, Rev Environ Contam Toxicol. 242 (2017) 61–104. [PubMed: 27718008]

[20]. Xue HY, Liu S, Wong HL, Nanotoxicity: A key obstacle to clinical translation of siRNA-based nanomedicine, Nanomedicine. 9 (2014) 295–312. [PubMed: 24552562]

[21]. Lauritzen L, Brambilla P, Mazzocchi A, Harsløf LB, Ciappolino V, Agostoni C, DHA Effects in Brain Development and Function, Nutrients. 8 (2016) 6.

[22]. Cardoso C, Afonso C, Bandarra NM, Dietary DHA and health: cognitive function ageing, Nutr Res Rev. 29 (2016) 281–294. [PubMed: 27866493]

[23]. Guerzoni LP, Nicolas V, Angelova A, In vitro Modulation of TrkB Receptor Signaling upon Sequential Delivery of Curcumin-DHA Loaded Carriers Towards Promoting Neuronal Survival, Pharmaceutical Research. 34 (2017) 492–505. [PubMed: 27995523]

[24]. Nguyen LN, Ma D, Shui G, Wong P, Cazenave-Gassiot A, Zhang X, Wenk MR, Goh EL, Silver DL, Mfsd2a is a transporter for the essential omega-3 fatty acid docosahexaenoic acid, Nature. 509 (2014) 503–506. [PubMed: 24828044]

[25]. Santos JR, Curran A, Navarro-Mercade J, Ampuero MF, Pelaez P, Pérez-Alvarez N, Clotet B, Paredes R, Moltó J, Simplification of Antiretroviral Treatment from Darunavir/Ritonavir Monotherapy to Darunavir/Cobicistat Monotherapy: Effectiveness and Safety in Routine Clinical Practice, AIDS Res Hum Retroviruses. 35 (2019) 513–518. [PubMed: 30909716]

[26]. Fonseca C, Moreira JN, Ciudad CJ, Pedroso de Lima MC, Simões S, Targeting of sterically stabilised pH-sensitive liposomes to human T-leukaemia cells, Eur J Pharm Biopharm. 59 (2005) 359–366. [PubMed: 15661509]

[27]. Narvekar M, Xue HY, Tran NT, Wong HL, A new nanostructured carrier design including oil to enhance the pharmaceutical properties of retinoid therapy and its therapeutic effects on chemo-resistant ovarian cancer, European Journal of Pharmaceutics and Biopharmaceutics. 88 (2014) 226–237. [PubMed: 24816129]

[28]. Keer HN, Kozlowski JM, Tsai YC, Lee C, McEwan RN, Grayhack JT, Elevated transferrin receptor content in human prostate cancer cell lines assessed in vitro and in vivo, J Urol. 143 (1990) 381–385. [PubMed: 1688956]

[29]. Zhao L, Pu SS, Gao WH, Chi YY, Wen HL, Wang ZY, Song YY, Yu XJ. Effects of HIV-1 tat on secretion of TNF-α and IL-1β by U87 cells in AIDS patients with or without AIDS dementia complex. Biomed Environ Sci. 27 (2014) 111–117. [PubMed: 24625401]

[30]. Lippi SLP, Craven KM, Hernandez CM, Grant GM, Flinn JM. Perfusion alters free zinc levels in the rodent brain.J Neurosci Methods. 315 (2019) 14–16. [PubMed: 30599147]

[31]. De Meyer S, Azijn H, Surleraux D, Jochmans D, Tahri A, Pauwels R, Wigerinck P, de Béthune MP, TMC114, a novel human immunodeficiency virus type 1 protease inhibitor active against protease-inhibitor resistant viruses, including a broad range of clinical isolates, Antimicrobial Agents Chemotherapy. 49 (2005) 2314–2321. [PubMed: 15917527]

[32]. Patel MM, Patel BM, Crossing the Blood-Brain Barrier: Recent Advances in Drug Delivery to the Brain, CNS Drugs. 31 (2017) 109–133. [PubMed: 28101766]

[33]. Yoshimura K, Current status of HIV/AIDS in the ART era, J Infect Chemother. 23 (2017) 12–16. [PubMed: 27825722]

[34]. Wu D, Si M, Xue HY, Wong HL, Nanomedicine applications in the treatment of breast cancer: current state of the art, Int. J. Nanomedicine. 12 (2017) 5879–5892. [PubMed: 28860754]

[35]. Fang CL, Al-Suwayeh SA, Fang JY, Nanostructured lipid carriers (NLCs) for drug delivery and targeting, Recent Pat Nanotechnol. 7 (2013) 41–45. [PubMed: 22946628]

[36]. Sharma G, Thakur K, Raza K, Singh B, Katare OP, Nanostructured Lipid Carriers: A New Paradigm in Topical Delivery for Dermal and Transdermal Applications, Crit Rev Ther Drug Carrier Syst. 34 (2017) 355–386. [PubMed: 29199589]

[37]. Meital LT, Windsor MT, Perissiou M, Schulze K, Magee R, Kuballa A, Golledge J, Bailey TG, Askew CD, Russell FD, Omega-3 fatty acids decrease oxidative stress and inflammation in macrophages from patients with small abdominal aortic aneurysm, Sci Rep. 9 (2019) 12978.

[38]. Candela P, Gosselet F, Saint-Pol J, Sevin E, Boucau MC, Boulanger E, Cecchelli R, Fenart L, Apical-to-basolateral transport of amyloid-β peptides through blood-brain barrier cells is mediated by the receptor for advanced glycation end-products and is restricted by P-glycoprotein, J Alzheimers Dis. 22 (2010) 849–859. [PubMed: 20858979]

[39]. Mulik RS, Bing C, Ladouceur-Wodzak M, Munaweera I, Chopra R, Corbin IR, Localized delivery of low-density lipoprotein docosahexaenoic acid nanoparticles to the rat brain using focused ultrasound, Biomaterials. 83 (2016) 257–268. [PubMed: 26790145]

[40]. Loughrill E, Thompson S, Owusu-Ware S, Snowden MJ, Douroumis D, Zand N, Controlled release of microencapsulated docosahexaenoic acid (DHA) by spray-drying processing, Food Chemistry. 286 (2019) 368–375. [PubMed: 30827620]

[41]. Shao K, Zhang Y, Ding N, Huang S, Wu J, Li J, Yang C, Leng Q, Ye L, Lou J, Zhu L, Jiang C, Functionalized nanoscale micelles with brain targeting ability and intercellular microenvironment biosensitivity for anti-intracranial infection applications, Adv Healthc Mater. 4 (2015) 291–300. [PubMed: 25124929]

[42]. Hishikawa D, Valentine WJ, Iizuka-Hishikawa Y, Shindou H, Shimizu T, Metabolism and functions of docosahexaenoic acid-containing membrane glycerophospholipids, FE BS Lett. 591 (2017) 2730–2744.

[43]. Puglia C, Bonina F, Effect of polyunsaturated fatty acids and some conventional penetration enhancers on transdermal delivery of atenolol, Molecules. 25 (2019) pii: E128.

[44]. Wu YN, Wang SL, Wang YC, et al., Reversal effect of docosahexaenoic acid on taxol resistance in human ovarian carcinoma A2780/T cells, Obstetrics & Gynecology International Journal. 1 (2014) 70–76.

[45]. Torres-Vergara P, Penny J, Pro-inflammatory and anti-inflammatory compounds exert similar effects on P-glycoprotein in blood-brain barrier endothelial cells, J Pharm Pharmacol. 70 (2018) 713–722. [PubMed: 29492971]

[46]. Fujimoto H, Higuchi M, Watanabe H, Koh Y, Ghosh AK, Mitsuya H, Tanoue N, Hamada A, Saito H, P-glycoprotein mediates efflux transport of darunavir in human intestinal Caco-2 and ABCB1 gene-transfected renal LLC-PK1 cell lines, Biol Pharm Bull. 32 (2009) 1588–1593. [PubMed: 19721237]

[47]. Wang JZ, Xiao N, Zhang YZ, Zhao CX, Guo XH, Lu LM, Mfsd2a-based pharmacological strategies for drug delivery across the blood–brain barrier, Pharmacological research. 104 (2016)124–131. [PubMed: 26747400]

[48]. Ben-Zvi A, Lacoste B, Kur E, Andreone BJ, Mayshar Y, Yan H, Gu C, Mfsd2a is critical for the formation and function of the blood-brain barrier, Nature. 509 (2014) 507–511. [PubMed: 24828040]

[49]. Andreone BJ, Chow BW, Tata A, Lacoste B, Ben-Zvi A, Bullock K, Deik AA, Ginty DD, Clish CB, Gu C, Blood-Brain Barrier Permeability Is Regulated by Lipid Transport-Dependent Suppression of Caveolae-Mediated Transcytosis, Neuron. 94 (2017) 581–594. [PubMed: 28416077]

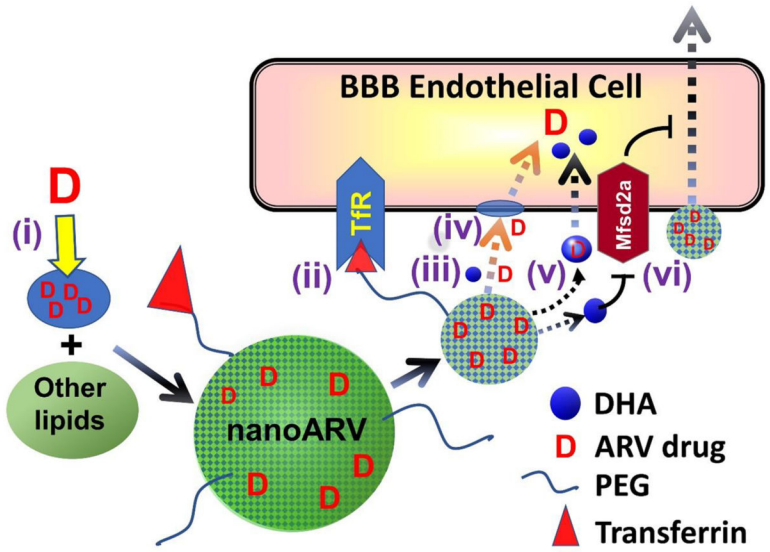

Figure 1.

Hypothetical strategies for a DHA-based lipid nanocarrier (nanoARV) to enhance delivery of antiretroviral (ARV) drug (*e.g.* duranavir) across the blood-brain barrier (BBB): (i) Efficient solubilization of lipophilic ARV drug molecules in DHA for improved drug dispersion andencapsulation (note: the DHA oil likely just gets finely or molecularly dispersed and mixed with other lipids instead of forming distinct micro-compartments); (ii) NanoARV can be further decorated with transferrin (Tf) to target Tf-receptor for improved BBB targeting(iii) The DHA content in nanoARVs facilitates more complete release of the drug; (iv) Any released DHA may help fluidizing the cell membrane of BBB endothelial cells to facilitate ARV drug diffusion; (v) Released DHA may possibly help a portion of the released drug to exploit active transport mechanisms of DHA such as Mfsd2a for additional improvement of cellular drug uptake; (vi) DHA may potentially de-inhibit the suppressive function of Mfsd2a against transcytotic transport.

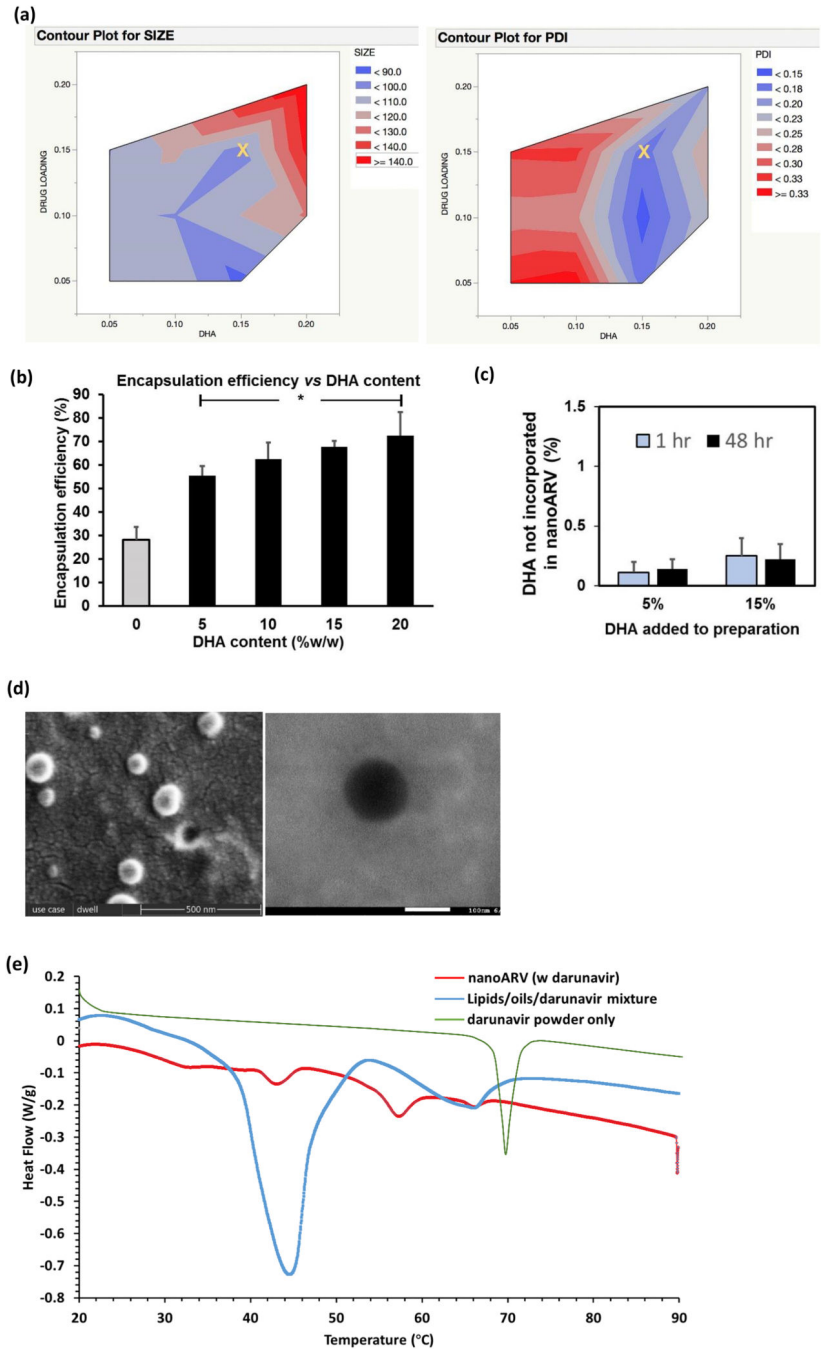

Figure 2.

Physical properties of nanoARVs. (A) Impact of DHA content and drug loading on nanocarrier diameter (left) and polydispersity index (PDI) of nanocarriers (right).The yellow X in each contour graph marks the amounts of DHA and darunavir (15% DHA; 15% intended darunavir payload) most typically used to prepare nanoARVs in the subsequent experiments.(B) Impact of DHA content on darunavir encapsulation efficiency in nanoARV. (C) Quantification of the amount of DHA not encapsulated in nanoARVs (5 or 15% w/w DHA added in preparation. NanoARVs stored at 4 °C). (D) Representative images of SEM

(left) and TEM (right) of Tf-nanoARV (15% DHA, 12% darunavir, Tf:lipids=1:10) are shown. (E) Differential scanning calorimetry thermogram of 15%DHA-nanoARVs (12% darunavir) and comparison with darunavir powder and lipids/drug mixture (the first heating run was used for nanoARVs and mixture; second run for darunavir powder). Means+SD (N=3) are shown. *P<0.01 *vs* no DHA

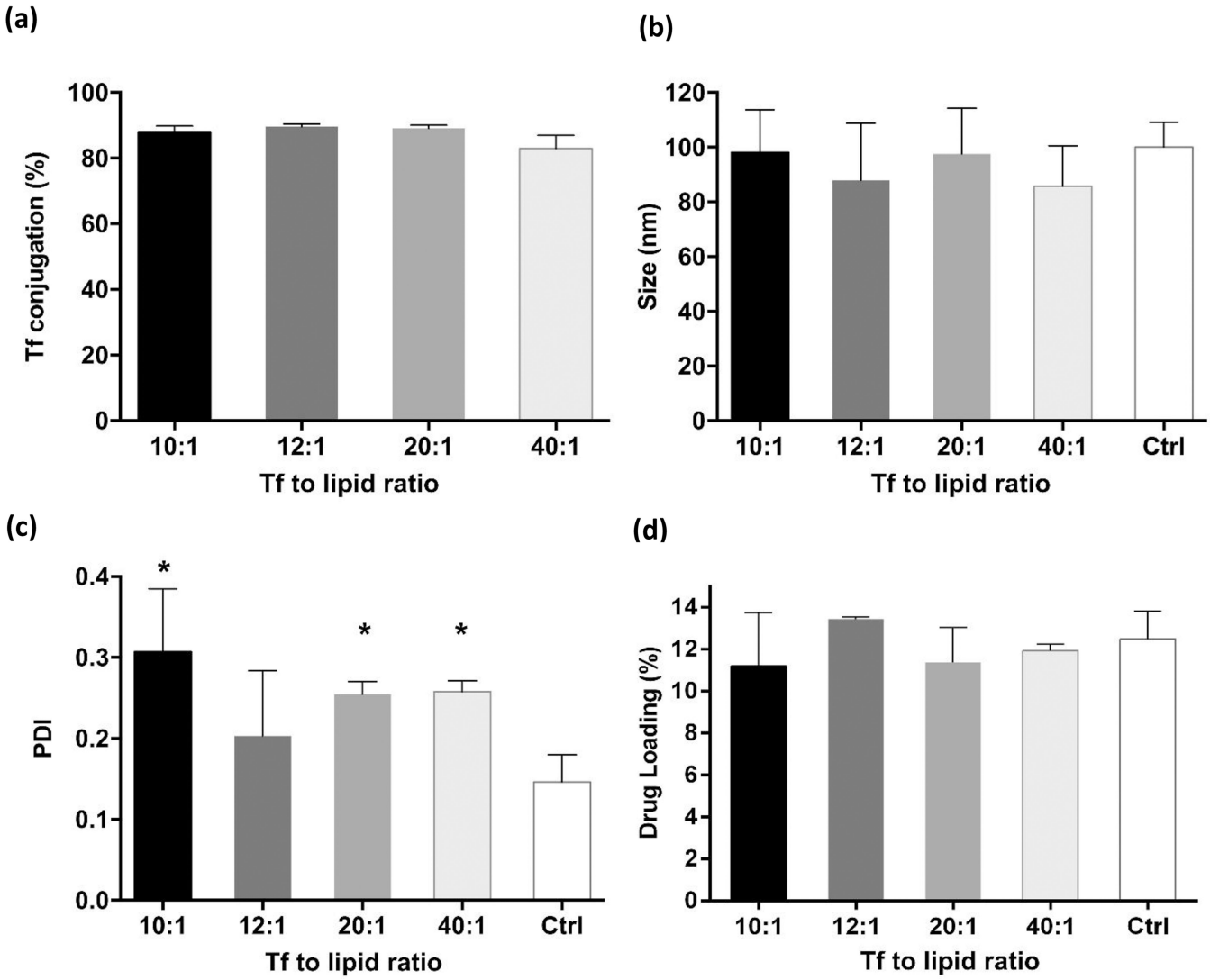

Figure 3.

Effects of transferrin (Tf)-decoration on various properties of nanoARVs, including: (A) Tf conjugation efficiency; (B) size of nanoARVs; (C) PDI of nanoARVs; (D) actual darunavir payloadMeans+SD (N=4) shown. *P<0.05 *vs* control

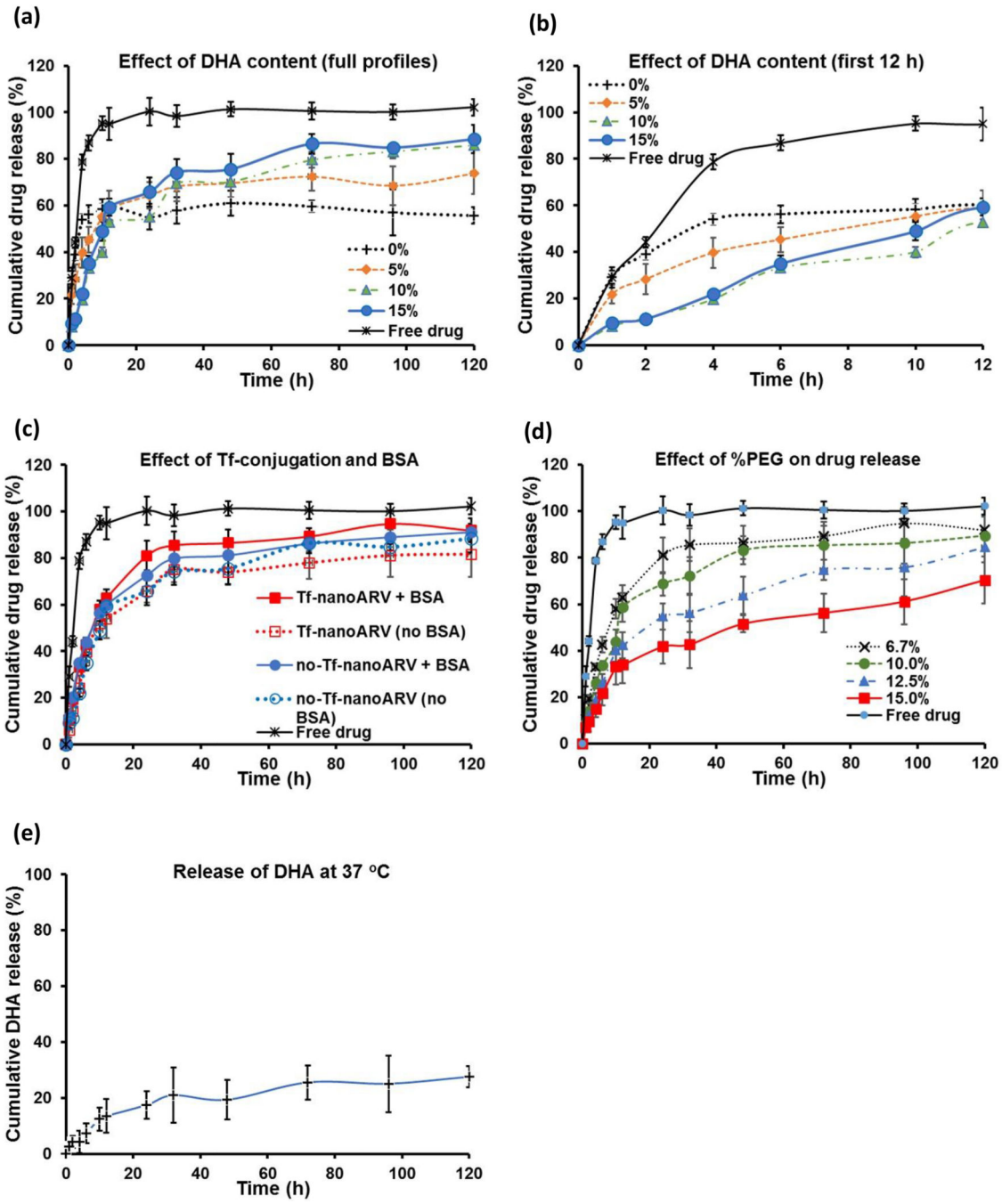

Figure 4.

Studies of release profiles. The effects of: (A) and (B) % DHA in nanoARVs, (C) Tf-conjugation and bovine serum albumin supplement (1% w/v BSA), and (D) % of DSPE-PEG2000 in nanoARVs on darunavir release are shown. (E) shows the release profile of DHA from nanoARVs. (B) highlights the first 12-hour portions of the full profiles shown in (A). All forms of nanoARVs used in (C) to (E) contained 15% DHA. The lipids to Tf ratio used in the Tf-nanoARV in (C) was 12:1. All studies performed in PBS at pH 7.2 and 37 °C.Means±SD (N=4) shown.

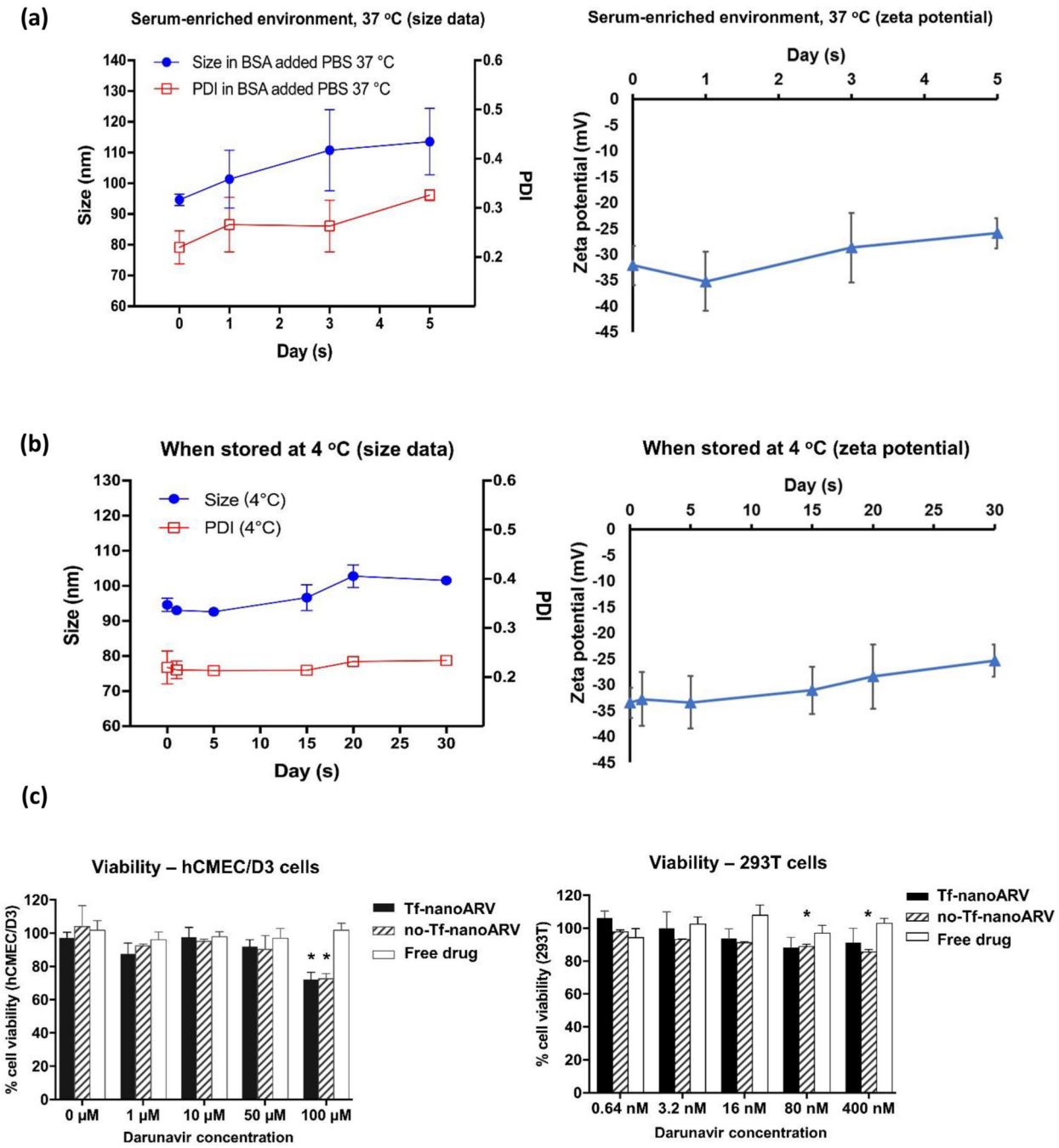

Figure 5.

Physical stability and cellular toxicity of nanoARVs. (A) Dispersion stability in BSA-supplemented buffer at 37 °C. (B) Storage stability of nanoARV in its stock suspension when refrigerated at 4 °C. In each of them the left panel presents the size data and the right panel presents the zeta potential data. (C) Viability of hCMEC/d3 cells (left panel) and 293T cells (right panel) after nanoARV treatment. Means±SD shown in (A) and (B) and Means +SD in (C). N=3 in each group. **P*<0.05 when compared with the viability of vehicle-treated cells.

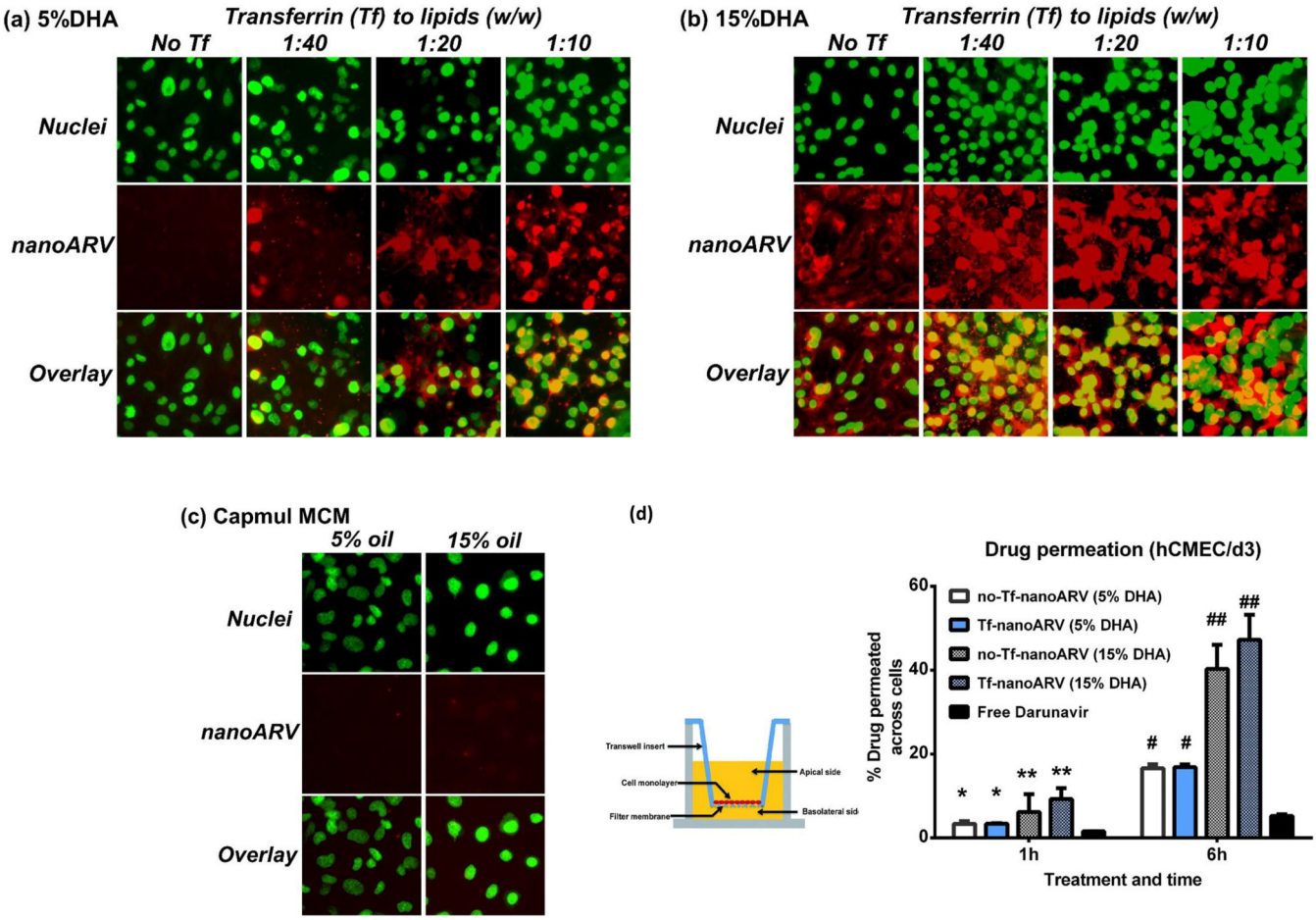

Figure 6.

Cellular uptake of nanoARVs into and permeation of its darunavir payload across hCMEC/d3 BBB models. (A) and (B) present cellular uptake of nanoARVs (in red) with different levels of DHA (A: 5%, B: 15%) and Tf-decoration (left to right: without Tf to Tf:lipid ratio = 1:10). Cell nuclei stained with DAPI (in green) to show their location of the cells. (C) shows cellular uptake of nanoARV incorporating 5% or 15% Capmul MCM C8 instead of DHA for comparison (no Tf conjugation). (D) presents quantitative result of darunavir that permeated across the hCMEC/d3 monolayer grown in transwell inserts by different nanoARV formulations. Means+SD (N=3) shown. * P<0.05 for 5%DHA *vs* free drug; ** P<0.05 for 15% DHA *vs* 5% DHA and P<0.01 for 15% DHA *vs* free drug; # P<0.01 for 5% DHA *vs* free drug; ## P<0.01 for 15% DHA *vs* both 5% DHA and free drug.

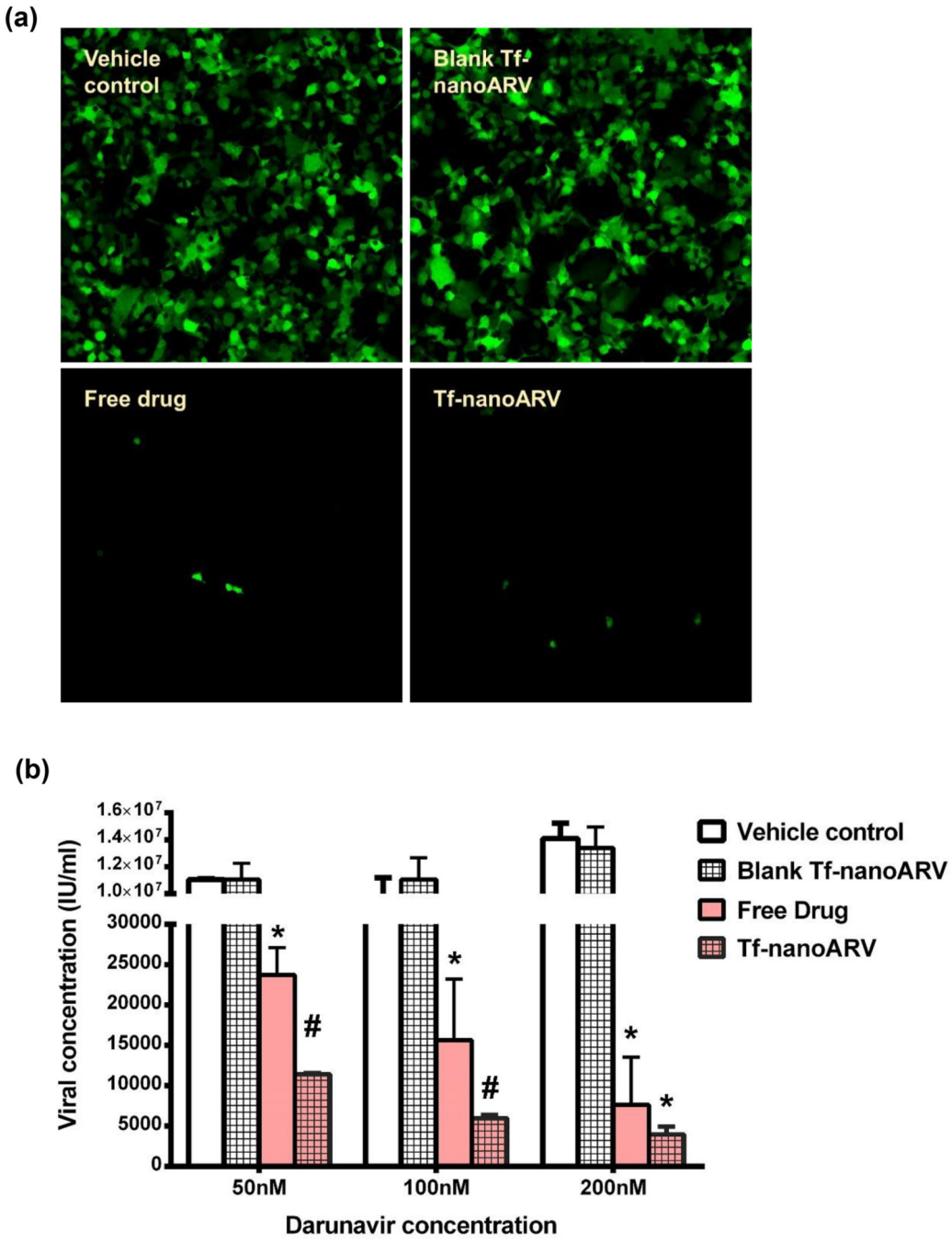

Figure 7.

Evaluation of anti-HIV activity of nanoARVs. (A) Effect on silencing the reporter gene expressing GFP (in green). (B) Suppression of production of HIV capsid protein p24 titer. 15% DHA-Tf-nanoARV was used. Means+SD (N=3) are shown. *P<0.01 *vs* vehicle control and blank Tf-nanoARV; #P<0.01 *vs* vehicle control, blank nanoARVs and free drug.

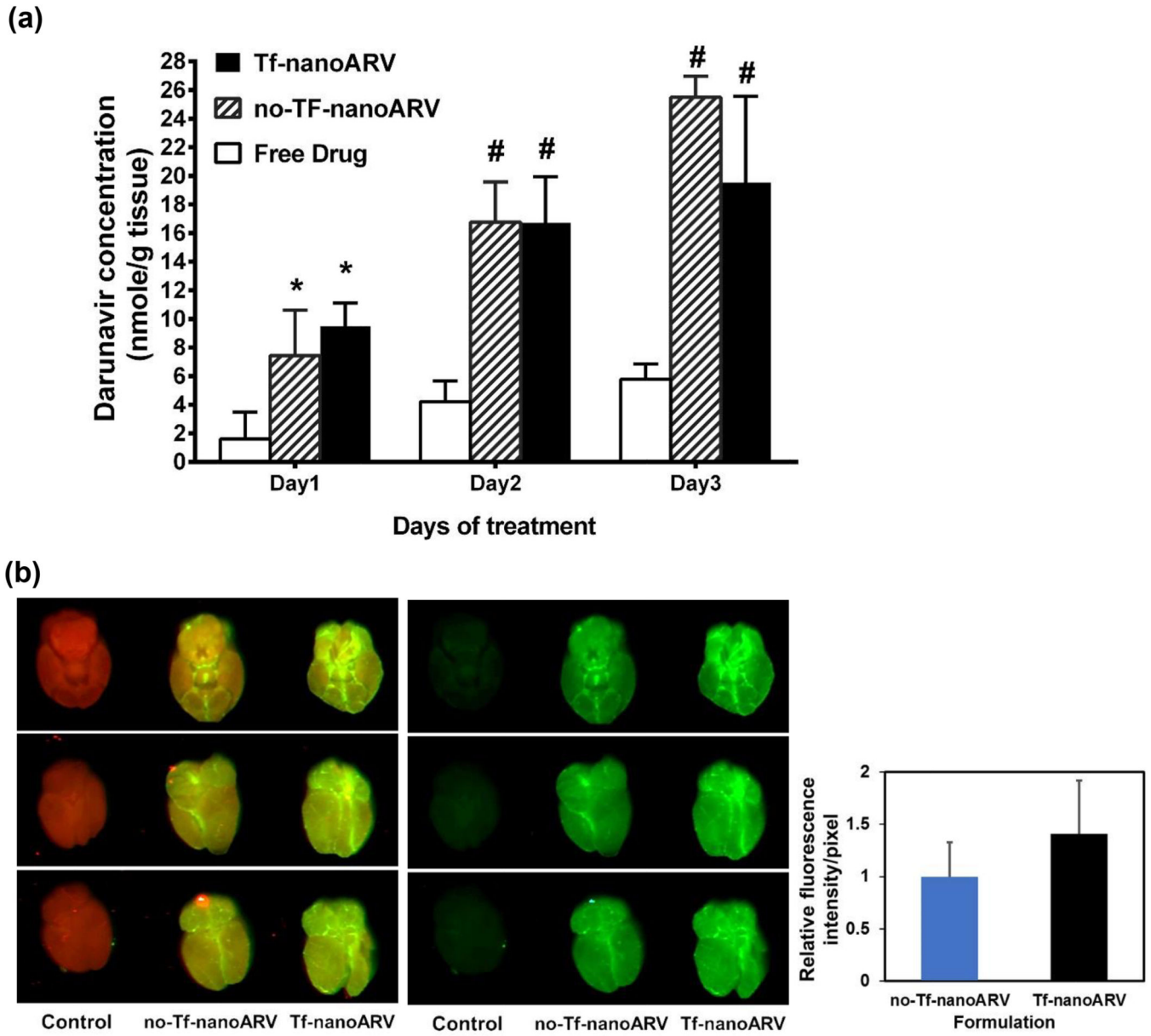

Figure 8.

Studies of *in vivo* accumulation of (A) darunavir and (B) nanoARVs in mice brains. In (B), nanoARVs were labeled with NIR dye and shown in green (brain tissue in red). Left panel shows the overlay, middle panels shows the nanoARVs only, and right panel compares the relative fluorescence intensity between no-Tf-nanoARV and Tf-nanoARV. Means+SD (for A: N=4 per time point, male and female equal ratio; for B, N=3, male only) are shown. * $P<0.05$ *vs* free drug; # $P<0.01$ *vs* free drug

Table 1.

Solubilities of darunavir in oils at 25 °C and nanoARVs prepared using DHA or Capmul MCM C8

Oil tested[#]	Darunavir solubility (mg drug/ mg oil)	Nanocarrier size (nm)	Polydispersity index (PDI)
Mineral oil	0.00076 ± 0.00046[$]	N.A.	N.A.
Triolein	0.017 ± 0.010	N.A.	N.A.
Soy bean oil	0.0034 ± 0.0025	N.A.	N.A.
Castor oil	0.082 ± 0.046	N.A.	N.A.
DHA	0.31 ± 0.13	w Cholesterol[^]: 93.02±4.33	0.197±0.003 [*]
		w Tripalmitin: 85.51±6.38	0.242±0.016
Capmul MCM C8	1.23 ± 0.55	w Cholesterol: 84.62±6.64	0.241±0.026
		w Tripalmitin: 67.11±2.31	0.291±0.013

[#] All oils used are in USP grade.

[$] all values in this table expressed as means ± S.D. (n=3).

[^] All nanoARVs made with 15% DHA/Capmul + cholesterol/tripalmitin, DSPC, DSPE-mPEG2000 at a molar ratio of 8:6:1.

[*] $P<0.05$ *versus* all other groups